

BEARING CONDITION DIAGNOSTICS VIA VIBRATION AND ACCOUSTIC EMISSION
MEASUREMENTS

J. Shiroishi, Y. Li, S. Liang, T. Kurfess, S. Danyluk
The GWW School of Mechanical Engineering
Georgia Institute of Technology
Atlanta, Georgia

Professor Thomas R. Kurfess

The George W. Woodruff School of Mechanical Engineering

Georgia Institute of Technology

Atlanta, GA 30332-0405

U.S.A.

ABSTRACT

This paper investigates defect detection methodologies for rolling element bearings through sensor signature analysis. Specifically, the utility of a new signal processing combination of the High Frequency Resonance Technique (HFRT) and Adaptive Line Enhancer (ALE) is investigated. Two transducers, the accelerometer and the acoustic emission sensor, are used to acquire data for this analysis. Experimental results have been obtained for inner race and outer race defects. Results show the potential effectiveness of the signal processing technique to determine both the severity and location of a defect.

The HFRT utilizes the fact that much of the energy resulting from a defect impact manifests itself in the higher resonant frequencies of a system. Demodulation of these frequency bands through usage of the envelope technique is then employed to gain further insight into the nature of the defect while further increasing the signal to noise ratio. If periodic, the defect frequency is then present in the spectra of the enveloped signal.

The ALE is used to enhance the envelope spectrum by reducing the broadband noise. It provides an enhanced envelope spectrum with clear peaks at the harmonics of a characteristic defect frequency. It is implemented by using a delayed version of the signal and the signal itself to decorrelate the wideband noise. This noise is then rejected by the adaptive filter that is based upon the periodic information in the signal [1].

Results have been obtained for inner race and outer race defects. They show the effectiveness of the methodology to determine both the severity and location of a defect. In two specific instances, a linear relationship between signal characteristics and defect size is indicated for accelerometer analysis.

1. INTRODUCTION

Bearings are of paramount importance to almost all forms of rotating machinery, and are among the most common of machine elements. As a consequence of their importance and widespread use, bearing failure is also one of the foremost causes of breakdown in rotating machinery. In fact, it is so important to machine maintenance and automation process that research on the cause and analysis of bearing failure has been conducted for four decades [2].

Ball and roller bearings have three components that typically experience damage. They are the rolling element, inner race, and outer race. The signature produced varies according to the damaged component and whether or not the impact location is in a loaded zone of the bearing. It has been shown that defect signatures are enhanced by the amount of loading in the area of impact [3]. This makes the signature potentially harder to recognize. A defect present on a rotating component produces periodic pulses that depend on the load characteristic of the system, with the largest pulses originating in the peak of a loaded zone. A defect on a stationary race in a loaded zone is intuitively easiest to detect, with a pulse of constant frequency (assuming constant rotational velocity) and higher magnitude.

Most difficulties posed in bearing initial fault detection stem from the presence of a variety of noises and the wide spectrum of a bearing defect signal. Therefore, the success of bearing fault detection methods usually depends on increasing a bearing defect signal-to-noise ratio. Identification and quantification of key signal features dictating the condition of the element is then the main priority.

To date, most work only serves to identify the presence of a defect, or at best differentiate based on qualitative measures such as light, medium, or heavy damage without practical,

quantitative grounds for fault identification [4-11]. There has been a deficiency in the development of a relationship between various detection methodologies and defect size. A defect becomes a failed bearing when an applicable definition of failure has been satisfied. For example, a defect that has reached a size of 0.0645 mm^2 (0.01 in.^2) is commonly defined to be a failure by industry standards [12]. To date, the development of such a diagnostic capability that lends itself to possible prognostics has not been addressed.

The methodology presented here serves to address these issues. First, the signal-to-noise ratio is greatly increased through processing. This allows defects of smaller magnitude to be detected, well before failure occurs. Second, results indicate a direct relationship between signal features and defect size, yielding a diagnostic tool that can be used to effectively quantify the defect.

2. SIGNAL PROCESSING METHODOLOGY

In this work, an adaptive line enhancer (ALE) is used to increase the detectability of a periodic defect signal. It enhances the spectrum of the envelope signal provided to it by the high frequency resonance technique (HFRT). Figure 1 displays a block diagram of the signal flow for the overall processing scheme. The HFRT takes advantage of the large amplitudes of a defect signal in the range of a high frequency system resonance, and provides a demodulated signal with a high defect signal-to-noise ratio in the absence of low frequency mechanical noise. The ALE is expected to reduce wideband noise of the obtained demodulated signal and, therefore, enhance the envelope spectrum of the defect signal with clear peaks at the harmonics of the characteristic defect frequency.

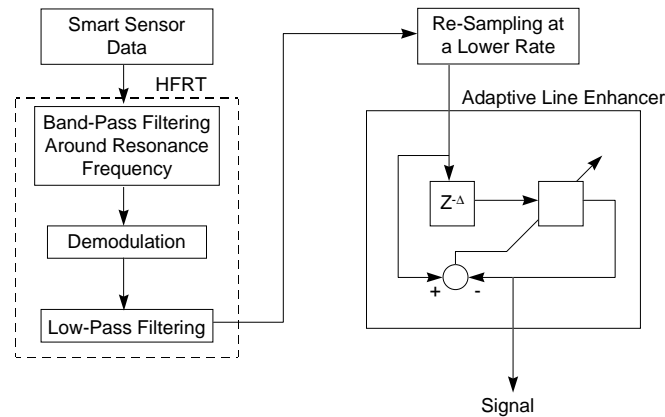


Figure 1. Signal Processing Diagram.

2.1 HIGH FREQUENCY RESONANCE TECHNIQUE

A bearing defect signal $s(t)$ can be represented by bursts of exponentially decaying sinusoidal vibration at a system resonant frequency f_r [13]. The high frequency resonance technique [14, 15] is illustrated in Figure 1 and Figure 2 and involves 3 steps. First, bandpass a measured signal (Figure 2 (a)) around a selected high frequency band with the center at a chosen resonant frequency of system, resulting in Figure 2 (b). Second, demodulate the bandpassed signal with a non-linear rectifier, resulting in Figure 2 (c). Third, use a low pass filter to cancel high frequency components and retain the low frequency information associated with bearing defects, resulting in Figure 2 (d)

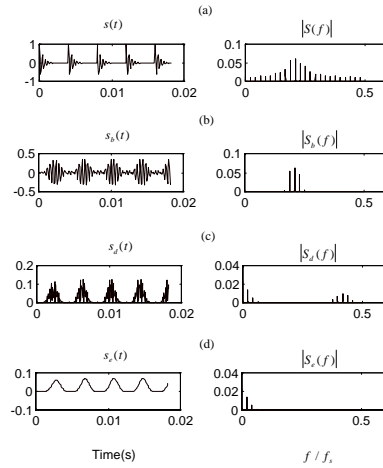


Figure 2. High Frequency Resonance Technique Processing.

In order to cancel the high frequency components and retain the low frequency information associated with a bearing defect, $s_d(t)$ is passed through a low pass filter. A pure bearing defect signal, $s(t)$ has nonzero magnitude only at the harmonics of a characteristic defect frequency. Therefore, the spectrum of $s_e(t)$ will have nonzero values only at the harmonics of the characteristic defect frequency that are less than the bandwidth of a used bandpass filter shown in Figure 2(d). The nonzero values of an envelope spectrum at the harmonics of a particular characteristic defect frequency indicate the occurrence of a defect, and the location of the defect can be determined by its unique defect frequency.

2.2 ADAPTIVE LINE ENHANCER

The envelope signal of a damaged bearing obtained by the above method is contaminated by broad band noise making it difficult to detect the early damage of the bearing. A real time

envelope signal $x(k)$ can be considered as the sum of narrow band signals $s_e(k)$ spaced at the harmonics of a characteristic defect frequency but corrupted by broad band noise $n(k)$.

$$x(k) = s_e(k) + n(k) \quad (1)$$

Therefore, the adaptive line enhancer (ALE) can be used to separate the narrow band signals from the broad band noise. ALE was first introduced by [1] and its performance was studied by [16]. The delayed version of $x(k)$ is used as the reference input of an adaptive filter. The output of the filter is then subtracted from the primary input signal $x(k)$ to form an error sequence $e(k)$. The error sequence is fed back to adjust the filter weights, shown in Figure 1.

The principle of the adaptive line enhancer can be understood as follows. The delay of an input signal causes the decorrelation between the broad band noise components of reference input and primary input while the narrow band signal is still highly correlated. To minimize the error power of the filter, the adaptive filter compensates for the correlated signal so that it can be canceled at the summing junction. Since the filter can not compensate for the decorrelation of the broad band noise components, only the narrow band signal is output from the adaptive filter. In the frequency domain, the filter weights will tend to form a bandpass function about the center frequencies of the narrow band input components. Therefore, the broad band noise components of delayed input are rejected while the narrow band signal information is retained. Here a recursive least mean squares (LMS) algorithm is used for this adaptive filter because of its computational simplicity. The output of the filter is:

$$y(k) = \mathbf{W}_k^T \mathbf{X}_k \quad (2)$$

where \mathbf{W}_k^T is the weight vector of the filter and input vector \mathbf{X}_k is

$$\mathbf{X}_k = [x(k-\Delta) \quad x(k-1-\Delta) \quad \cdots \quad x(k-L+1+\Delta)]^T \quad (3)$$

L is the length of the filter. Then the error is:

$$e(k) = x(k) - y(k) \quad (4)$$

The mean square error (MSE) is the expected value of $e(k)$. The LMS algorithm controls the weight vector of the filter so that the mean square error is minimized. The optimal weight vector \mathbf{W}^* that minimizes the MSE is

$$\mathbf{W}^* = R^{-1}P \quad (5)$$

where the input signal autocorrelation vector P is

$$P = E\{x(k)\mathbf{X}_k^T\} \quad (6)$$

and the autocorrelation matrix R is:

$$R = E\{\mathbf{X}_k\mathbf{X}_k^T\} \quad (7)$$

[1].

In practice, R and P are generally unavailable because they require an expectation operation (E). The following recursive LMS algorithm is a practical method to find an approximate solution of equation (5). The weights of the filter are updated by:

$$\mathbf{W}_{k+1} = \mathbf{W}_k + 2\mu e(k)\mathbf{X}_k \quad (8)$$

where μ is adaptive step size. The simulation results show that it is appropriate to let μ satisfy the following stability condition in practice [17].

$$0 < \mu < \frac{1}{L\{\text{power of input}\}} \quad (9)$$

The LMS algorithm is outlined as follows:

Step 1. Generate delayed version $x(k - \Delta)$ of input signal $x(k)$.

Step 2. Form the input vector X_k defined in equation (3).

Step 3 . Calculate the output of the filter $y(k)$ by equation (2).

Step 4. Calculate the output error $e(k)$ by equation (4).

Step 5. The weight vector is updated by equation (8).

Step 6. Go back to Step 1.

Therefore, given the input sequence $x(k)$ and initial value of the weight vector, the values of filter output $y(k)$, the error $e(k)$ and the weight vector W_k can be computed for all time by equations (2), (4), and (8).

Without the requirement of a priori information, the ALE's self-tuning capability allows it to find weak narrow band signals such as multiple sinusoids in wide band noise. The ability to separate two closely spaced lines by the ALE is determined by the length of the finite impulse response (FIR) filter. The detectability of a sinusoidal signal by the ALE given in [1] is:

$$(\text{number of data samples}) * (\text{SNR}/8) \quad (10)$$

where SNR is signal-to-noise ratio. Therefore the ALE has the potential to detect the line spectrum of a defect bearing HFRT signal in a noisy environment. Figure 7 subplots 3 and 4 illustrate the enhanced line spectrum by the ALE.

2.3 DEFECT DETERMINATION

Given that defect location and the shaft speed together with bearing geometry dictate the frequency of impact generation, it is a simple matter to calculate these frequencies. The Timken

LM501310 cup and LM501349 cone were chosen for all testing. This is a tapered roller bearing with a bore diameter of 41.275 mm (1.625 in.) and an outer diameter of 73.4314 mm (2.8910 in.). At 1200 RPM this yields defect frequencies of 164.64 Hz for a cup defect, and 215.36 Hz for a cone defect. These frequencies are often the focus of frequency domain analysis techniques, and are also critical to the combination of the HFRT and ALE presented in this work.

A peak ratio (P.R., equation (11)) is defined as the sum of the peak values of the defect frequency, and harmonics, over the average value of the spectrum.

$$P.R. = \frac{N^* \sum_{j=1}^n P_h}{\sum_{k=1}^N A_i} \quad (11)$$

P_h is the amplitude value of the peak located at the defect frequency harmonic, A_i is the amplitude at any frequency, and N is the number of points in the spectrum. The number of harmonics in the spectrum, n , is found by $600/f_d$. Six hundred is used as the maximum frequency in the analyzed spectrum, and f_d is the characteristic defect frequency. The peak ratio is a dimensionless ratio determined for damaged and undamaged bearings, and is only used to indicate the presence of a defect. Then, the peak value of the first harmonic after HFRT is used to determine the magnitude of the defect. Therefore, once the peak ratio verifies that a defect is present, the peak value is then used to estimate the size of the defect. The effectiveness of the peak ratio is compared to that of other standard detection methods of kurtosis, RMS, and crest factor. This is done in the frequency domain after HFRT. Thus, all analyses and comparisons will be drawn from the same data sets after similar processing.

3. TEST SYSTEM

A schematic of the test system can be seen in Figure 3. A four bearing system is contained within a test housing. A Wilcoxon 736T high frequency accelerometer is used to acquire vibration signals, and a Physical Acoustic Corporation type R15 acoustic emission sensor is used to detect high frequency stress waves. The resulting AE signal from the processor (ALM8) is a demodulated version that is very similar to a raw signal processed by the HFRT technique.

A Krohn-Hite #3384 programmable filter is used to prevent aliasing, and low pass filters the accelerometer data at 10 kHz (half the sampling frequency). The acoustic emission data are low pass filtered at 1 kHz because the ALM 8 already envelopes the signal.

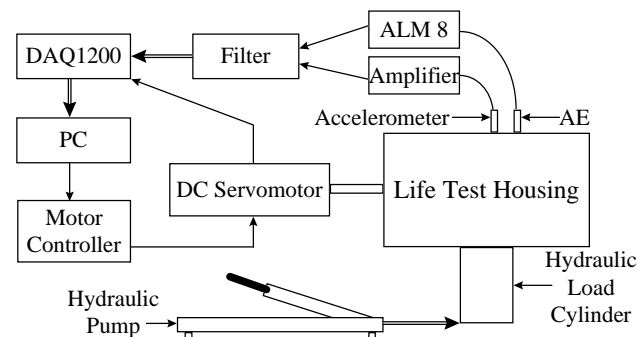


Figure 3. Experimental Schematic.

Since the premise of the HFRT technique is based upon proper selection of a resonant frequency band, the resonances of the bearing test system had to be determined. Several distinct bands were located through hammer impact testing, and experimentation revealed that the band between 7.5 and 9.2 kHz is more readily excited by defect impacts. Therefore, it is the focus of attention for accelerometer analysis.

4. EXPERIMENTAL RESULTS AND CONCLUSIONS

In the testing, all damage takes the form of scratches made to the center of the raceways with a diamond scribe. All cup and cone scratches are controlled as to a length of approximately 2.54 mm (0.1 in.). The width of the damage created is controlled by the number of passes that a scribe makes over the raceway. The defect widths examined range from 15.40 μm to 408.48 μm . It is useful to note that all of these defect sizes are well below industry standards for the definition of a failure, as mentioned earlier. The filter length L of 200, adaptive step size μ of 0.001 and delay Δ of 5 in the ALE routine were used in the experiments.

4.1 OUTER RACE DEFECTS

Seven bearings of damage levels ranging from 0.00 μm to 349.32 μm are examined. The most significant result obtained from outer race damage experiments is the determination of a relationship between peak value and defect width for accelerometer data. These results were obtained under 1200 RPM and 4911 N/bearing loading conditions. At least four data sets for each condition were taken. The tabulated averages of these experiments are found in Table 1. Figure 4 shows the relationship between peak value and defect width. All seven defect sizes appear on the graph because the peak ratio was able to determine the presence of defects in all cases. This can be seen from the table where the peak ratios for defective bearings are substantially higher than that for the good bearing. The vertical variation for a given defect size represents a confidence interval for measurements. Thus, in practice, a given peak value measurement has a window of accuracy in defect width prediction. Moreover, the y-intercept

represents the noise level of the system. This directly affects sensitivity, which for this system lies somewhere between a defect of width 0.00 μm and 15.40 μm .

Unlike the peak value, the traditional signal features of RMS, kurtosis, and crest factor values do not follow a consistent trend. While the RMS and kurtosis values actually follow a generally increasing pattern (Figure 5 and Figure 6), neither follow a continuously increasing pattern. Crest factor appears to be completely uncorrelated, randomly increasing and decreasing. It is possible that the resolution of these methods is insufficient to detect such small changes in defect size.

Table 1. 1200 RPM Accelerometer Experiments for Cup Damage.

Defect Width (μm)	RMS (g)	Kurtosis	Crest Factor	P.R. with ALE	P.R. w/o ALE	Peak Value (g)
0.00	0.0051	3.025	4.228	12.85	5.78	9.70×10^{-5}
15.40	0.0046	3.220	4.473	156.95	17.81	2.12×10^{-4}
38.03	0.0051	5.141	5.319	238.78	64.17	8.66×10^{-4}
75.40	0.0071	5.065	5.421	255.38	59.36	1.00×10^{-3}
104.92	0.0068	5.168	5.165	281.49	58.84	1.28×10^{-3}
111.87	0.0103	5.620	5.664	238.33	49.21	1.52×10^{-3}
349.32	0.0172	7.137	4.719	252.14	112.77	3.88×10^{-3}

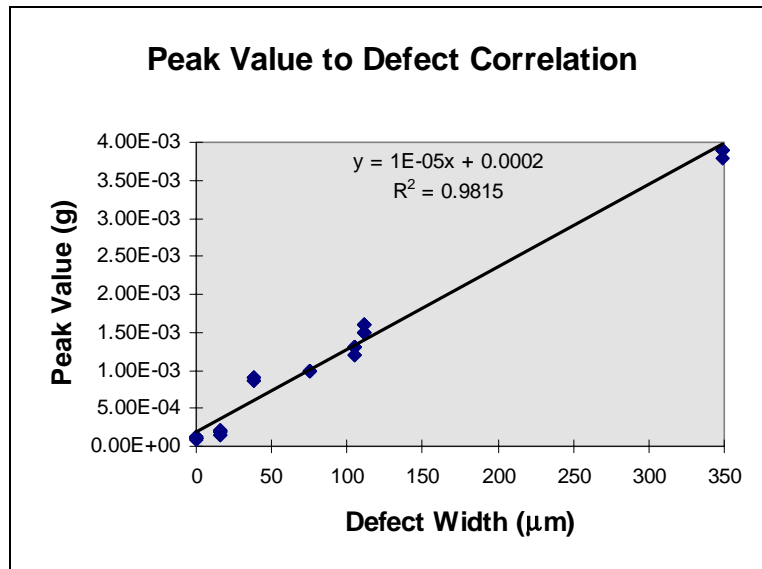


Figure 4. Peak Value Relationship for Cup Damage, 1200 RPM.

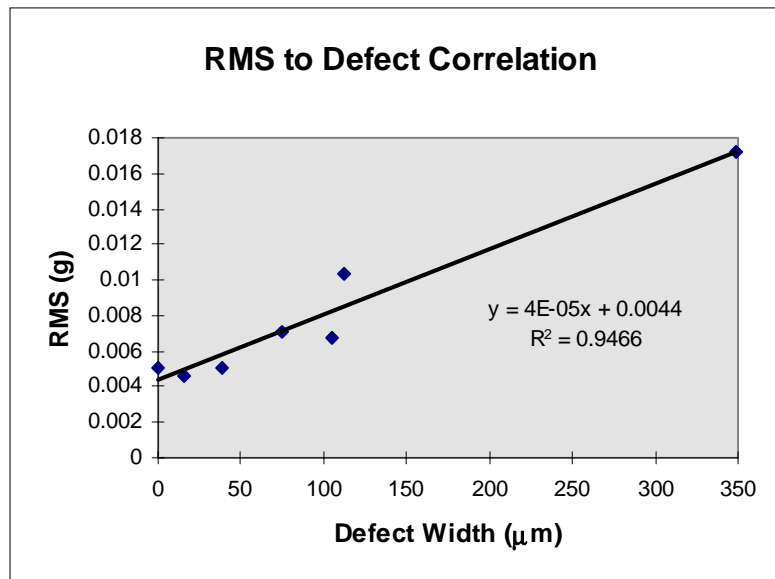


Figure 5. RMS Relationship for Cup Damage, 1200 RPM.

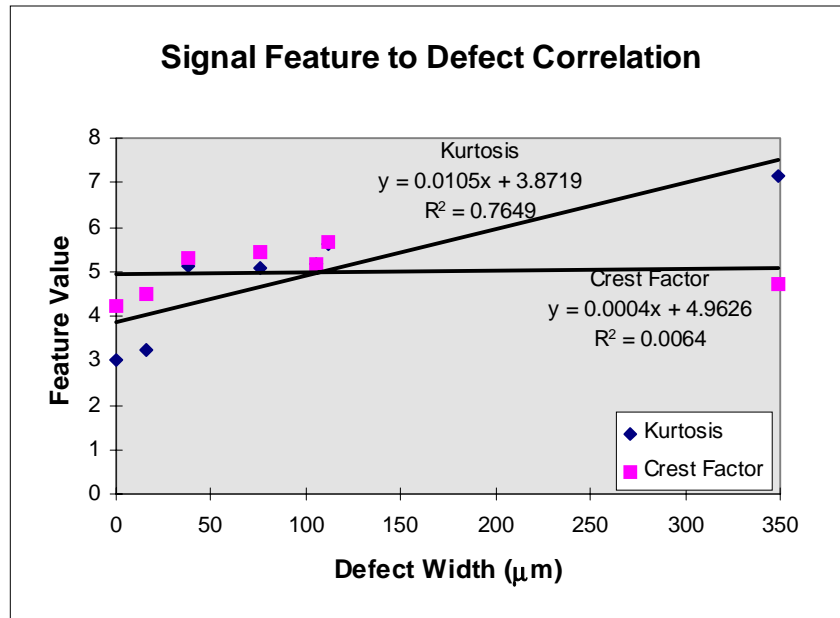


Figure 6. Crest Factor and Kurtosis Relationship for Cup Damage, 1200 RPM.

Figure 7 and Figure 8 show results of analysis for 15.40 μm and 349.32 μm damage. These plots give raw data, raw spectrum, HFRT spectrum, and HFRT with ALE spectrum. The defect frequencies and related harmonics are quite clear at 164 Hz and higher. It is clear from the plots that the defect frequency becomes more prominent as damage increases, even to the point that it is visible in the raw time signal. Moreover, the advantage of the ALE routine is clearly seen in Figure 7, where the defect peaks become quite prominent after noise cancellation.

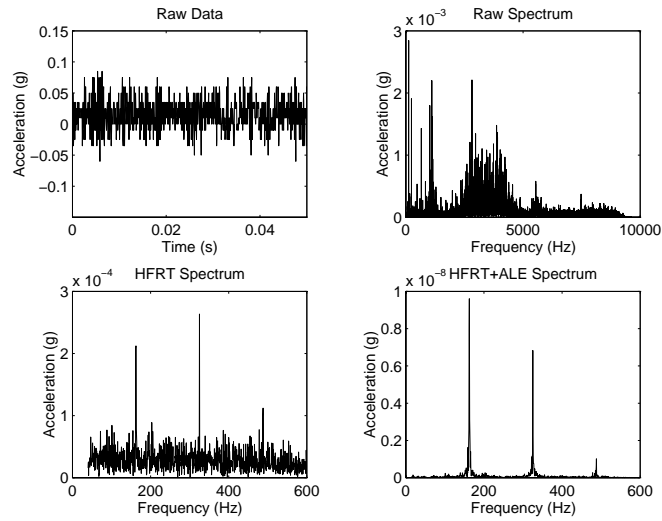


Figure 7. Accelerometer Data Analysis for 15.39 μm Cup Scratch at 1200 RPM.

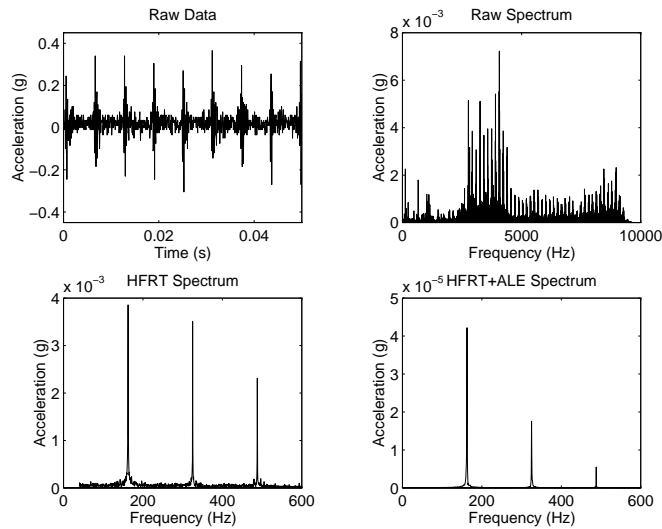


Figure 8. Accelerometer Data Analysis for 349.32 μm Cup Scratch at 1200 RPM.

The AE data were taken simultaneously under exactly the same conditions. Figure 9 shows results of AE data processing for a heavy 349.32 μm cup defect. While an increased peak value trend was observed, no clear linear relationship exists in this case. Table 2 lists calculated averages for this AE data. The smallest defect detected was 38.03 μm . As expected, in all cases

when the peak ratio indicates a defect, the peak value is increased. However, the increased peak value does not follow an increasing trend, except to say that its levels are elevated. Additionally, for this speed, the acoustic emission sensor is not as sensitive as the accelerometer, whose detected sensitivity is 15.39 μm . However, when the AE does detect a defect, it is clearly identified, with the peak ratio increasing an order of magnitude. Moreover, RMS, kurtosis, and crest factor follow no clear trend. In fact, they do not even experience significantly elevated levels as with the peak value.

Table 2. 1200 RPM AE Experiments for Cup Damage.

Defect Width (μm)	RMS (g)	Kurtosis	Crest Factor	P.R. with ALE	P.R. w/o ALE	Peak Value (g)
0.00	0.0372	3.272	4.910	22.66	8.03	2.50×10^{-5}
15.40	0.0278	3.059	4.326	21.90	8.49	8.16×10^{-6}
38.03	0.0694	4.304	4.111	258.17	89.97	7.90×10^{-3}
75.40	0.0631	3.901	4.323	251.36	64.91	4.18×10^{-3}
104.92	0.0356	3.667	4.438	217.40	38.90	3.57×10^{-4}
111.87	0.0673	3.763	4.375	234.28	51.41	3.28×10^{-3}
349.32	0.1431	4.418	4.418	266.69	113.48	3.79×10^{-2}

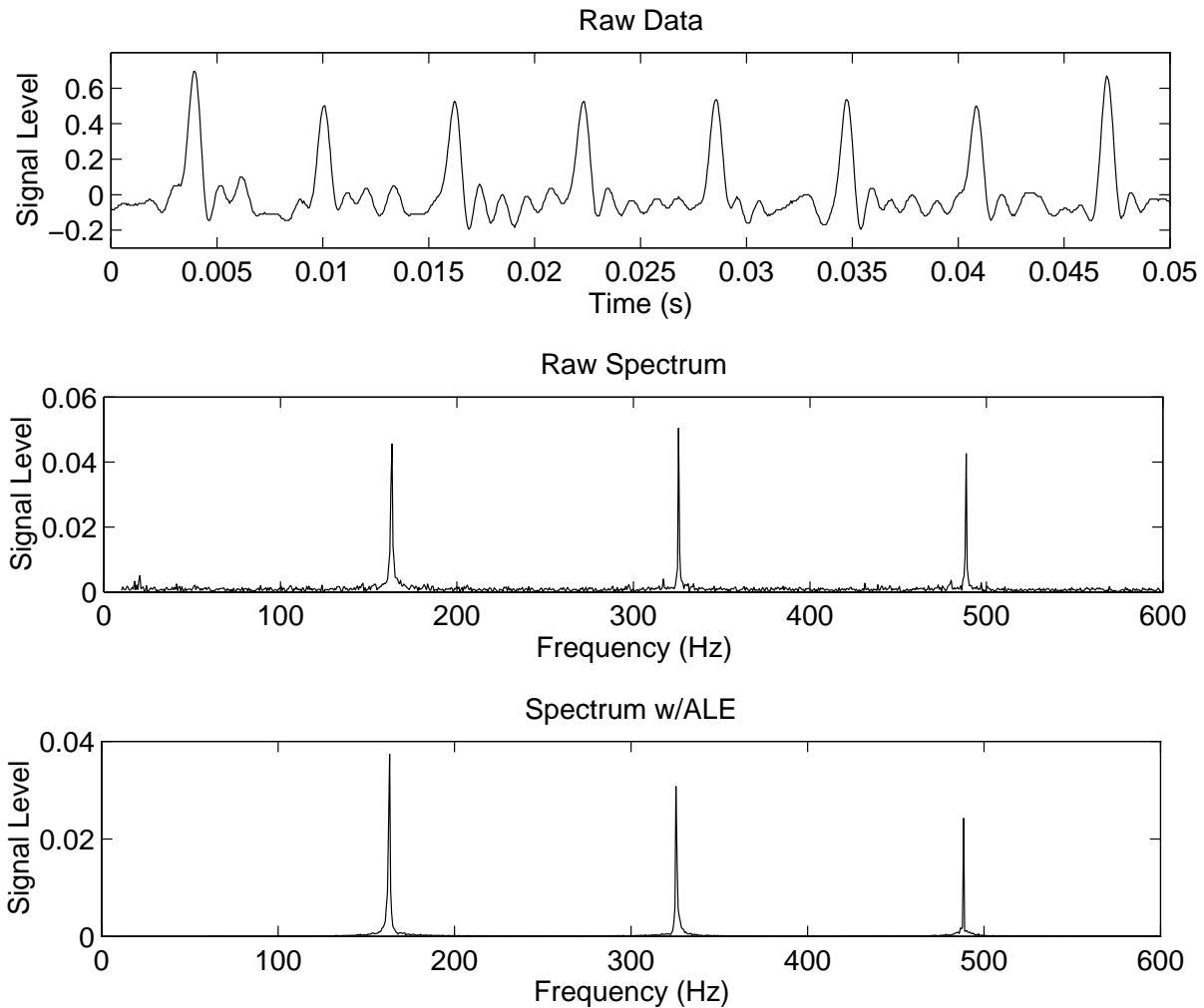


Figure 9. AE Analysis for Cup Damage.

Additionally, several conclusions can also be drawn by comparing the ability of the accelerometer and AE sensor. The accelerometer is more sensitive to cup defects than the AE sensor. The ability of each method is slightly diminished using the AE sensor, with the crest factor becoming insensitive. Given that the RMS does tend to increase, crest factor fails because the peak value of the time signal does not increase commensurately. Another observation is that

typically the shaft speed (20 Hz) is clearer in the AE signal. This may be useful in verifying the speed, and thereby raising confidence in defect frequency calculations and conclusions.

4.2 INNER RACE DEFECTS

Experiments were conducted on bearings with six different levels of inner race (cone) damage. Table 3 shows the average results of this testing at 1200 RPM. The most interesting outcome is the relationship found between peak value and defect width. This is seen in Figure 10 where a linear fit has been done to illustrate this relationship. However, as seen in the table, the peak ratio does not indicate the presence of a defect for the first defect width. As a result, these data do not appear on the linearization plot. As with the cup defect, the noise level can be seen reflected in the y-intercept, and a vertical window of uncertainty surrounds each defect prediction as a result of variation in test results.

From the table, it is clear that RMS is not correlated to defect size. However, kurtosis, crest factor, and the peak ratio are, but neither are related as closely as the peak value. This can be seen in Figure 11, where linear fits are performed for both kurtosis and crest factor. The variances for both are higher than for peak ratio, although the kurtosis fit is reasonable.

Table 3. 1200 RPM Accelerometer Analysis for Cone Damage

Defect Width (μm)	RMS (g)	Kurtosis	Crest Factor	P.R. w/ALE	P.R. w/o ALE	Peak Value (g)
0.00	0.0051	3.028	4.288	9.23	4.77	9.03×10^{-5}
34.57	0.0081	3.024	4.372	9.41	4.85	1.34×10^{-4}
43.28	0.0070	3.186	4.822	17.84	6.04	1.70×10^{-4}
81.46	0.0074	3.499	5.171	71.59	10.90	3.13×10^{-4}
104.62	0.0070	4.217	5.880	49.96	10.27	3.59×10^{-4}
408.48	0.0103	6.334	6.733	55.44	16.73	8.37×10^{-4}

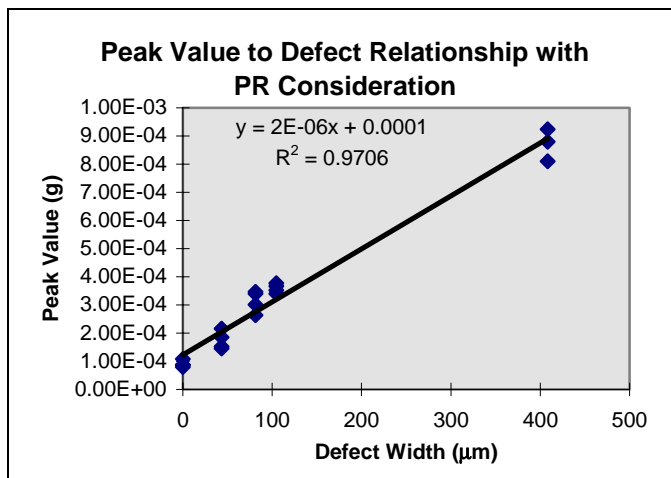


Figure 10. Accelerometer Relationship for Cone Defects with PR Consideration.

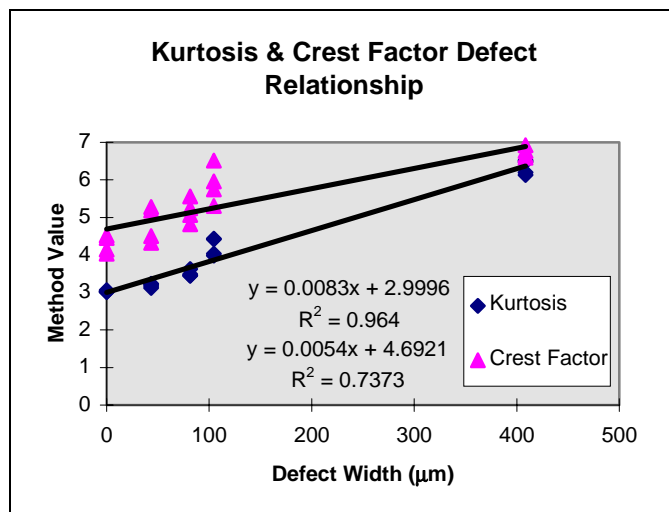


Figure 11. Kurtosis and Crest Factor to Defect Relationship for Cone Defects.

The rotational frequency is easily identified for this defect type. This is because the defect is on the rotating race and revolves relative to the load region at 20 Hz. This results in not only the defect frequency of 215.36 Hz, but beat frequencies at 20 Hz on either side of the characteristic defect frequency. There are even 40 Hz and 60 Hz harmonics of the rotational

frequency present. All of these features can be seen in Figure 12 and are clear in this case because the defect is large.

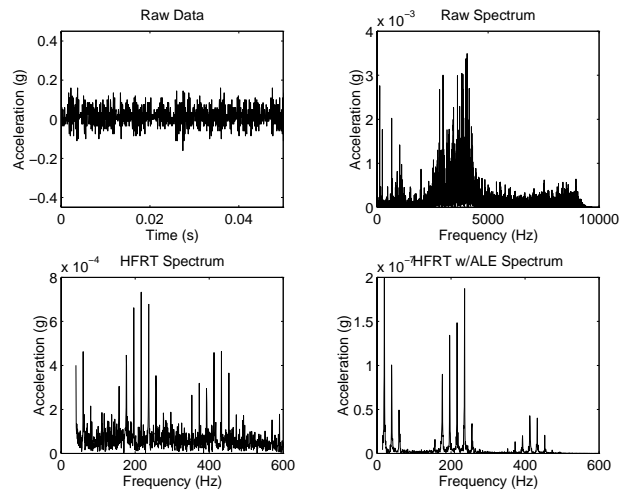


Figure 12. Accelerometer Analysis for 408 μm Cone Defects.

Analysis of the acoustic emission data reveals that the acoustic emission sensor is not sensitive to any of the cone defects tested. No defect frequencies are identified in any of the cases, not even for the heaviest cone defect. Since the impacts are of the same nature, it is reasonable to assume that the same type of strain induced stress waves are generated. However, none of these emissions are transmitted to the AE sensor at a level strong enough to be recognized. There are a few reasons why this is possible. AE signals generated by an inner race defect have to travel farther and through more interfaces than those for any other type of defect. Also, signal strength may be diminished if the line of travel for the AE wave is not direct to the sensor. This will be influenced by the line created by the position of the defect, the roller, and the sensor placement. Additionally, it is also reasonable to assume that the farther any signal must travel, the weaker it will get.

5. DISCUSSION

The ability of both the sensors and signal processing methods to detect and diagnose two specific types of defects under the given conditions has been demonstrated. Overall, the accelerometer is comparable to or better than the AE sensor at detecting the defect types. The sensors are better able to detect outer race defects, but the AE sensor was not sensitive to the inner race defects tested.

The peak ratio is the most reliable indicator of localized defect presence out of the methods tested. It enjoys greater or equal success in every case. Kurtosis and RMS are a close second in their reliability. Crest factor is quite insensitive, being the most unreliable method tested. It failed to show a correlation to defect size in each case.

Moreover, after defect detection by the peak ratio, the peak value demonstrates a good correlation to defect size. A linear relationship between peak value and defect width of the accelerometer data at 1200 RPM has been outlined for both inner and outer race defects, with R^2 correlation values of 0.9815 and 0.9706 found for cup and cone relationships. To date, prior work has not attempted to establish such a relationship. All previous work located has focused on the identification of the presence of a defect, with possible size differentiation based on categories such as light, medium, and heavy.

It is important to note that while the peak ratio excels at localized defect detection, it is not particularly capable of identifying other types of damage. Debris denting is a case in point because of the lack of a characteristic defect frequency. Results show that either sensor used with the RMS technique has the ability to differentiate between the good, light, and heavily debris dented bearings. Kurtosis and crest factor both failed for this case.

Kurtosis is a statistical measure based on the shape of the waveform. A good bearing with a random distribution of asperities has a theoretical kurtosis value of three, regardless of amplitude of the signal. A bearing with debris denting is essentially the same thing as a good bearing, only with asperities on a larger scale. Therefore the signal level is increased, and the kurtosis values remain unchanged. The crest factor values do not increase because they are based on the peak value of the time signal over the RMS level. It is true that the peak value of the time signal increases as increased debris denting takes place. However, since the RMS value also increases significantly the ratio of the two tends to remain the same, and crest factor gives no indication of a defect.

Therefore, a comprehensive defect detection scheme should incorporate the methodologies most effective in diagnosing the defects of interest. While the frequency based peak ratio is excellent for localized defect detection, a time domain method such as RMS is more suited for non-localized defect detection such as debris denting or insufficient lubrication.

ACKNOWLEDGEMENTS

This work was funded by the Office of Naval Research under research grant number N00014-95-10539, entitled “Integrated Diagnostics.” The Timken Company and The Torrington Company have provided valuable support as well. Any opinions, findings, and conclusions or recommendations are those of the author and do not necessarily reflect the views of the Office of Naval Research, The Timken Company, or The Torrington Company.

BIBLIOGRAPHY

1. B. Widrow et al. 1975 Proceedings of the IEEE v63 n12, 1692-1716, Adaptive Noise Canceling: Principles and Applications.
2. O.G. Gustaffson and T. Tallian 1962 ASME Transactions v5, 197-209, Detection of Damage of Assembled Rolling Element Bearings.
3. R. Monk 1972 Process Engineering v53, 135-137, Vibration Measurement Gives Early Warning of Mechanical Faults.
4. R.J. Alfredson and J. Mathew 1985 The Institution of Engineers, Australia, Mechanical Engineering Transactions v10 n2, 102-107, Time Domain Methods for Monitoring the Condition of Rolling Element Bearings.
5. R.J. Alfredson and J. Mathew 1985 The Institution of Engineers, Australia, Mechanical Engineering Transactions v10 n2, 108-112, Frequency Domain Methods for Monitoring the Condition of Rolling Element Bearings.
6. M. Carney, A. Mann and J. Gagliardi 1994 Applied Acoustics v43, 333-351, Adaptive Filtering of Sound Pressure Signals for Monitoring Machinery in Noisy Environments.
7. A. Daadbin and J.C.H. Wong 1991 International Journal of Mechanical Engineering Education v19 n4, 295-304, Different vibration monitoring techniques and their application to rolling element bearings.
8. P.Y. Kim 1987 Journal of Propulsion and Power v3 n1, 84-89, Proximity Transducer Technique for Measuring Health Monitoring.
9. C.J. Li and J. Ma 1992 Sensors and Signal Processing for Manufacturing, ASME PED v55, 187-196, Bearing Localized Defect Detection Through Wavelet Decomposition of Vibrations.
10. H.R. Martin and F. Hornarvar 1995 Applied Acoustics v 44, 67-77, Application of Statistical Moments to Bearing Failure Detection.
11. K.F. Margin and P. Thorpe, 1992 Wear v159, 153-160, Normalised spectra in monitoring of rolling bearing elements.
12. D. Lawrentz 1996, The Timken Company, Canton OH.
13. S. Braun and B. Datner 1979 Journal of Mechanical Design Transactions v101, 118-125, Analysis of Roller/ball Bearing Vibrations.

- 14.P.D. Mcfadden and J.D. Smith 1984 Tribology International v17, 1-18, Vibration Monitoring of rolling Element Bearings by the High Frequency Resonance Technique-A Review
- 15.Y.-T. Su and S.-J. Lin 1992 Journal of Sound and Vibrations v155, 75-84, On Initial Fault Detection of a Tapered Rolling Bearing: Frequency Domain Analysis.
- 16.J.R. Treichler 1979 IEEE Transactions on Acoustics, Speech, and Signal Processing Vol. ASSP-27 n1, 53-62, Transient and Convergent Behavior of the Adaptive Line Enhancer.
- 17.P.M. Clarkson 1993 Optimal and Adaptive Signal Processing, 166-173, Boca Raton FL: CRC Press.